RESEARCH ARTICLE

Machine Learning Empowered Brain Tumor Segmentation and Grading Model for Lifetime Prediction

**M. RENUGADEVI[1], K. NARASIMHAN[1], C. V. RAVIKUMAR[2],
RAJESH ANBAZHAGAN[1], (Senior Member, IEEE), GIOVANNI PAU[3], (Member, IEEE),
KANNAN RAMKUMAR[1], MOHAMED ABBAS[4], N. RAJU[1], K. SATHISH[2],
AND PRABU SEVUGAN[5], (Senior Member, IEEE)**

[1]School of Electrical and Electronics Engineering, SASTRA Deemed University, Thanjavur 613401, India
[2]School of Electronics Engineering, Vellore Institute of Technology, Vellore 632014, India
[3]Faculty of Engineering and Architecture, Kore University of Enna, 94100 Enna, Italy
[4]Electrical Engineering Department, College of Engineering, King Khalid University, Abha 61421, Saudi Arabia
[5]Department of Banking Technology, Pondicherry University (A Central University), Puducherry 605014, India

Corresponding authors: K. Narasimhan (knr@ece.sastra.edu), Giovanni Pau (giovanni.pau@unikore.it), and C. V. Ravikumar (cvrkvit@gmail.com)

ABSTRACT An uncontrolled growth of brain cells is known as a brain tumor. When brain tumors are accurately and promptly diagnosed using magnetic resonance imaging scans, it is easier to start the right treatment, track the tumor's development over time, and select the best surgical techniques. This paper applies advanced and popular methods for preprocessing, segmentation, grading of tumors and lifetime prediction. On exploring various encoder-decoder architectures, UNet++ architecture was chosen for detecting brain tumor and obtained an accuracy of 98% and intersection over union score of 0.7483 during the testing phase. The segmented image is used to extract the radiomics features. Despite of several difficulties, data imbalance among the dataset is the common obstacle for survival prediction. To solve and increase the sample size and preserve the class distribution, the synthetic minority oversampling technique and adaptive synthetic approaches are used. After balancing the dataset, the important characteristics are selected using principal component analysis and tree-based feature selection techniques. The collected characteristics are used as input for machine learning techniques including stochastic gradient descent, decision tree, random forest, and support vector machine. The distinction between low-grade glioma and high-grade glioma is investigated as a binary classification. Accuracy, precision, recall, and F1score are used in the performance evaluation. The highest accuracy of 96% is achieved using stochastic gradient descent. Lifetime prediction of high-grade glioma patients is made using regression techniques: Linear, ridge, stochastic gradient descent, and extreme gradient boosting. We have obtained the least mean square error of 93726.45 using the extreme gradient boosting method. The proposed approach is contrasted with the most recent segmentation, grading, and lifetime prediction methods described in the literature.

INDEX TERMS Brain tumor, data imbalance, glioma, machine learning, data augmentation, UNet++.

I. INTRODUCTION

Brain tumors can be either non-cancerous or cancerous, with the former being benign and malignant [1]. These cells can

start in the brain or another area of the body and enlarge to the brain. The most frequent primary brain tumors that originate in supportive glial cells are known as Gliomas [2]. For distinguishing between various grades of gliomas, medical professionals refer to LGG (Low-Grade Glioma) and HGG (High-Grade Glioma) classifications [3], [4]. Tumors

that are fast-growing and aggressive are known as HGGs, while LGGs are tumors that proliferate slower.

MRI (Magnetic Resonance Imaging) is a critical imaging instrument that depicts gliomas' phenotypic and intrinsic heterogeneity for diagnosis, treatment planning, and tracking the tumor's reaction to therapy. It can provide minute details about the tumor's size, position, and features [5], [6]. Fluid-Attenuated Inversion Recovery (FLAIR), T2-weighted, T1-weighted, and diffusion-weighted imaging are some radiology sequences that can bring out specific variations in different regions of gliomas. These sequences are effective in highlighting diverse tissue characteristics.

Patients and their family members are severely impacted by a grave medical condition known as a brain tumor. To make well-informed decisions about care, it's crucial to comprehend the diagnosis, potential treatments, and prognosis. Predicting how long a patient with a brain tumor will survive is a complex procedure considering numerous factors. Brain tumor survival prognosis can be challenging, but it's crucial for developing appropriate treatment plans and ensuring optimal outcomes. In recent years, it's possible to predict brain tumor survival rates by implementing machine learning algorithms [7], [8]. The algorithms study massive patient information datasets to find patterns used for survival predictions. Brain tumor survival prediction using machine learning algorithms involves training models on relevant features to estimate the likelihood of a patient's survival [9].

Early diagnosis of the brain tumor is the most important factor to increase the survival rate. It also helps in the appropriate treatment, monitor the tumor's progression over time and decide on proper surgical methods. However, life time prediction is a critical task due to variability in tumor sizes or shapes, tumor identification, area computation, segmentation, classification, and discovering ambiguity in the segmented region. The motivation behind this research is to improve the outcome of the patient lifetime by enhancing the quality of treatment and care. The data imbalance among the dataset are solved with SMOTE (Synthetic Minority Oversampling Technique) and ADASYN (Adaptive Synthetic) methods which fine tunes the classification and prediction results of machine learning algorithms. The major phases involved in this work are brain tumor segmentation, grading and life time prediction. The contributions of this proposed paper are as follows:

- Initially, the BraTS2020 (Brain Tumor Segmentation) dataset are collected and preprocessed to make the MRI images appropriate for segmentation.
- The proposed framework incorporates the brain tumor segmentation using advanced and popular UNet++ architecture. Accuracy, precision, sensitivity, specificity IOU score and Jaccard Loss are metrics employed to the evaluation of segmentation.
- Radiomics features are extracted from the segmented image. SMOTE (Synthetic Minority Over-sampling Technique) and ADASYN (Adaptive Synthetic

Sampling) upsampling techniques are used to increase the samples.
- After applying Tree-Based and Principal Component Analysis (PCA) techniques, the selected features are used to build predictive machine learning classifiers, such as support vector machines (SVM), random forest method, decision tree and SGD (Stochastic Gradient Descent). The evaluation metrics such as precision, recall and F1-score are used.
- Finally, regression models such as linear, ridge, SGD, and Extreme gradient boost (XGBoost) are used to predict the overall survival of the brain tumor patients. Mean square error (MSE) and R-squared (R^2) metrics are used for evaluation.
- The results are compared with the alternate approaches mentioned in the literature and the superiority of the proposed framework.

The rest of this manuscript is organized as follows: the related previous work of this study is explained in Section II. The proposed method is explained in Section III with a dataset description and the metrics used for the evaluation. Section IV describes the experimental results and the comparison of the work. Finally, the conclusion and future work are given in Section V.

II. LITERATURE REVIEW

The task of completely automated segmentation of brain tumors in the field of medical image analysis is complex. It was introduced to overcome the difficulties of manual and semi-automated segmentation [10]. Initially, Long et al. implemented a Fully Convolutional Network (FCN) in 2015 for the semantic segmentation in which each pixel was labelled to the particular defined classes [11]. To achieve dense predictions at various spatial resolutions, FCN swaps out the fully connected layers in conventional Convolutional Neural Network (CNN) for convolutional layers. Several machine learning models were introduced and implemented using the BraTS Challenge brain tumor dataset.

UNet is well known adopted architecture explained by Ronneberger et al. in 2015 for biomedical image segmentation [12]. It involves an encoder pathway to capture context and also a similar decoder pathway for exact localization. The encoder and decoder are linked with skip connections, which assist in transmitting fine-grained details. The enhancement of the UNet architecture is Attention UNet, proposed by Oktay et al. in 2018 [13]. The added attention gates help to highlight important features and decrease irrelevant data during the fusion of features. As a result, Attention UNet is more efficient when medical image segmentation is considered [14].

Introducing the concept of residual learning with UNet, He et al. in 2015 proposed deep convolutional neural network architecture known as ResNet (Residual Network [15]. ResNet made waves in computer vision and paved the way for training intense neural networks with better

performance. Much other architecture has been built upon its fundamental building block, and it continues to inspire new deep-learning research. Further improving and adapting the algorithm, several variants such as GoogLeNet [16], ResNet-34 and ResNet-50 [17] have been proposed to address specific challenges in various domains and tasks. On the other hand, ResidualU-Net (ResUnet) uses a blend of the UNet and ResNet models by fusing residual connections. This model permits a straightforward exchange of information between the encoder and decoder pathways, tackling the vanishing gradient issue and increasing gradient propagation. Zhou et al. 2018 proposed another extension of the UNet architecture with a nested and dense skip pathway structure, UNet++ [18]. The UNet++ approach incorporates several nested U-shaped subnetworks within the UNet structure to construct a more intricate and intricate network. These subnetworks are composed of encoder-decoder pathways that are reminiscent of the UNet architecture, with the addition of further skip connections. Not only are connections inserted between the corresponding encoder and decoder blocks, but they are also established across different nested subnetworks.

These models are used for various applications. Loss functions and Optimizers are utilized to fine tune the performance of convolutional models for semantic segmentation. Data augmentation artificially expands the training dataset to make the model becomes more adaptable to new datasets through image manipulation techniques. The ultimate goal is to allow the model to study the generalization of unseen data. The training's optimizers and loss function have a significant impact on the model's performance. The dice loss and cross-entropy are frequently employed loss functions for semantic segmentation. Adam and SGD are the most commonly used optimizers.

After detecting the tumor region from the MRI brain images, relevant features must be extracted to guide clinical diagnosis and treatment. Robert et al. in 2016 introduced the concept of radiomics that aims to extract quantitative information to characterize tumors, determine treatment response and predict patient outcomes [19]. Kickingereder et al. explained the potential of radiomics in cancer research and emphasized the importance of tumor treatment from robust feature extraction methods [20]. Cho et al. [8] extracted the radiomics features from the MRI modalities and used for the glioma classification with machine learning classifiers such as support vector machine, logistics and random forest classifiers. This study utilized radiomics features extracted from MRI to discriminate between different subtypes of glioblastoma. Then the Tree-based and PCA methods were employed to choose the relevant features from the extracted radiomics features. The selected features were upsampled using the SMOTE [21] and ADASYN [22] techniques. These upsampled features were fed as input to the binary grading classifiers such as SVM, decision tree, random forest method and SGD [23], [24], [25]. This results in the classification of low-grade and high-grade gliomas. After applying PCA,

the selected features were given as input to linear regression, ridge, SGD and XGBoost regressor models to outcome the survival prediction of the brain tumor [25], [26], [27], [28], [29].

The inference from this detailed study implies that the previous work didn't the address the data imbalance problem which has to focus for the improvement of the accuracy and performance. Also, selecting the most important and relevant features play a vital role in the classification and prediction process using machine learning algorithms. These limitations are resolved using this proposed approach.

III. MATERIALS AND METHODS

The overall lifetime survival process includes preprocessing, segmentation of the images, PyRadiomics feature extraction, feature selection, classifications and predictions. Fig. 1 shows the overall brain tumor survival prediction process.

A. DATASET DESCRIPTION

In the domain of medical imaging, the Multimodal Brain Tumor Segmentation Challenge 2020 dataset, also known as BraTS2020, is a well-known standard for brain tumor segmentation and classification activities [26], [30]. It is the collection of brain MRI images using several modalities, such as FLAIR, T1, T2, and T1-CE (Contrast Enhanced) images. Fig. 2(a) shows the sample MRI image for each modality. Various information about the brain tumor are scanned and highlighted in a different modality. Each MRI modality is made up of 155 slices per volume. Segmentation annotation labels for the tumor sub-regions are categorized as 0 for background, 1 for Necrotic/Non-Enhancing tumor (NCR/NET), 2 for Peritumoral Edema (ED), and 4 for an Enhancing tumor (ET). BraTS2020 has training and testing subsets, with the former including 369 cases with ground truth annotations that identify the tumor parts of the brain scans. Conversely, the testing subset doesn't have any ground truth annotations and is explicitly used for testing and evaluating the performance of various models and algorithms.

B. DATA PREPROCESSING

The BraTS2020 dataset consists of four distinct MRI modalities such as T1, T2, T1_CE and FLAIR. These four images are considered as the input to the UNet++ architecture to train the model. This dataset image already underwent preprocessing steps, including the same anatomical template registration, exact resolution interpolation and skull-striping for brain tissue sectionalization. However, it is necessary to remove the extra black background from each MRI modality to improve the computing process time of the machine learning algorithms. Thus the dimension of each image is cropped from $240 \times 240 \times 155$ to $128 \times 128 \times 128$. Also, the data augmentation was done to increase the size of the dataset. Then the augmented dataset is divided as 80% for training, 10% for validation, and 10% for testing.
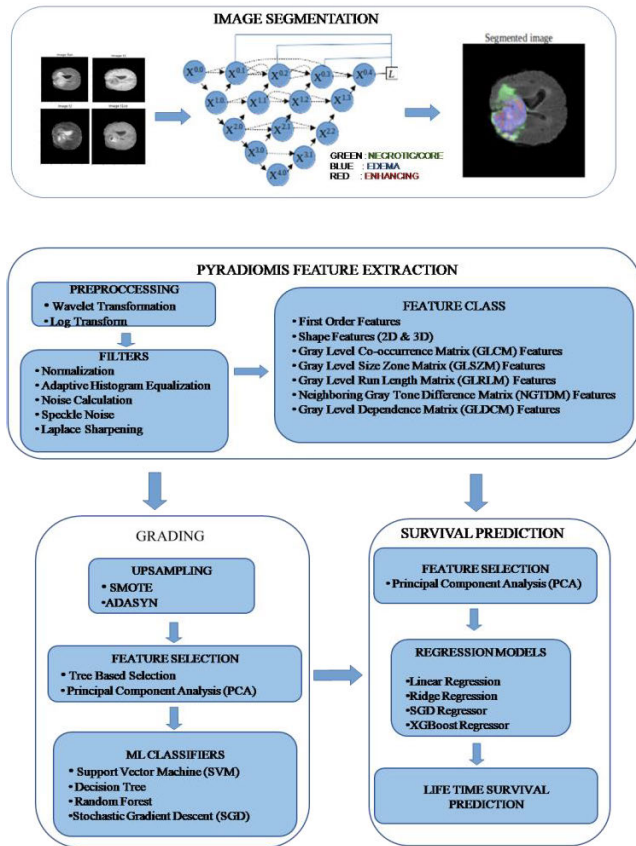
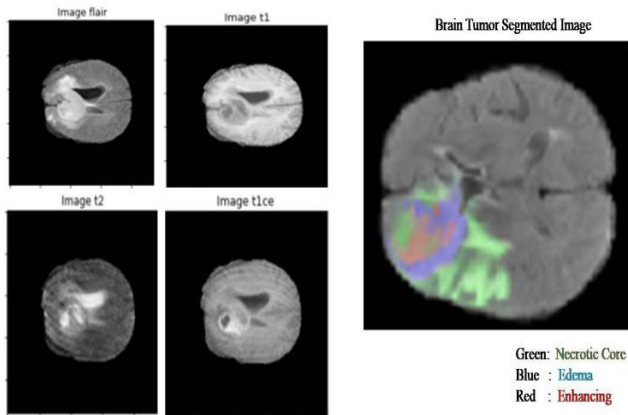**FIGURE 1.** Brain tumor segmentation, feature extraction, grading and lifetime survival prediction process.

FIGURE 2. (a) Sample MRI of FLAIR, T1, T1-CE, T2 images from BraTS2020 dataset. (b) UNet++ brain tumor segmented image with labels.

C. UNet++ ARCHITECTURE

In the realm of medical image analysis, UNet++ architecture favored deep learning for semantic segmentation tasks [18]. Essentially, the UNet++ structure is comprised of two core building blocks: the encoder and the decoder. The encoder component executes a contracting path, like the UNet, leading to each level down sampling the feature map's spatial resolution while intensifying channel numbers. Instead of

the traditional UNet decoder, UNet++ incorporates several nested

U-shaped subnetworks, each comprised of an encoder-decoder pair. Fig.3 shows the network architecture of the UNet++ model. The preprocessed images of size 128*128*128 are used as input for the training of the model. The contracting path involves two 3*3 kernel convolution with ReLu (rectified linear unit) as activation function. It is followed by max pooling with 2*2 kernel for downsample. In the extracting path 2*2 transposed convolution are carried out for upsampling the feature map and concatenated with contracting path convolution to enhance the feature map. As contrast to encoder path which decrease the feature map size and doubles the number of kernels, decoder path doubles the feature map size and halves the number of kernels at each layer. At the last layer, 1*1 convolution is employed with softmax activation function to get the segmented image. Introducing several modifications, UNet++ upstage U-Net through aspects such as:

1) NESTED DENSE SKIP CONNECTIONS

UNet++ improves segmentation accuracy by using nested dense skip connections that connect the encoder and decoder sub-networks at multiple levels as shown in the Fig 3 with dotted blue color arrows. This innovative approach significantly enhances the information flow between the two sub-networks.

2) DEEP SUPERVISION

By utilizing deep supervision, UNet++ encourages more detailed representations of input images by incorporating the output of every layer in the decoder sub-network into the loss calculation as indicated by red line in Fig 3. This leads to improvement of segmentation accuracy.

Using a series of convolutional layers and max-pooling layers, the encoder sub-network in UNet++ is built. Conversely, the decoder sub-network employs upsampling layers and convolutional layers. Multiple levels of nested dense skip connections connect the encoder and decoder sub-networks. To normalize data, a min-max scalar was used. The learning rate of 0.001 was employed with the Adam optimizer for training the model across 50 epochs. The batch size of 1 is selected to generalize the model well on both training and testing dataset. Table 1 shows the parameters used for training the model. This segmented MRI image using this architecture is shown in Fig. 2(b). The sub regions of the tumor were classified with different color modes as shown in the segmented MRI brain image. The green color depicts a Necrotic/Non-Enhancing tumor (NCR/NET), blue color shows Peritumoral Edema (ED), and red color displays Enhancing tumor (ET). Accuracy, IoU score and Jaccard Loss are the metrics used to evaluate the algorithm performances.

D. FEATURE EXTRACTION

Tumor or tissue characteristics can reveal valuable information for diagnostic, prognostic, and treatment planning
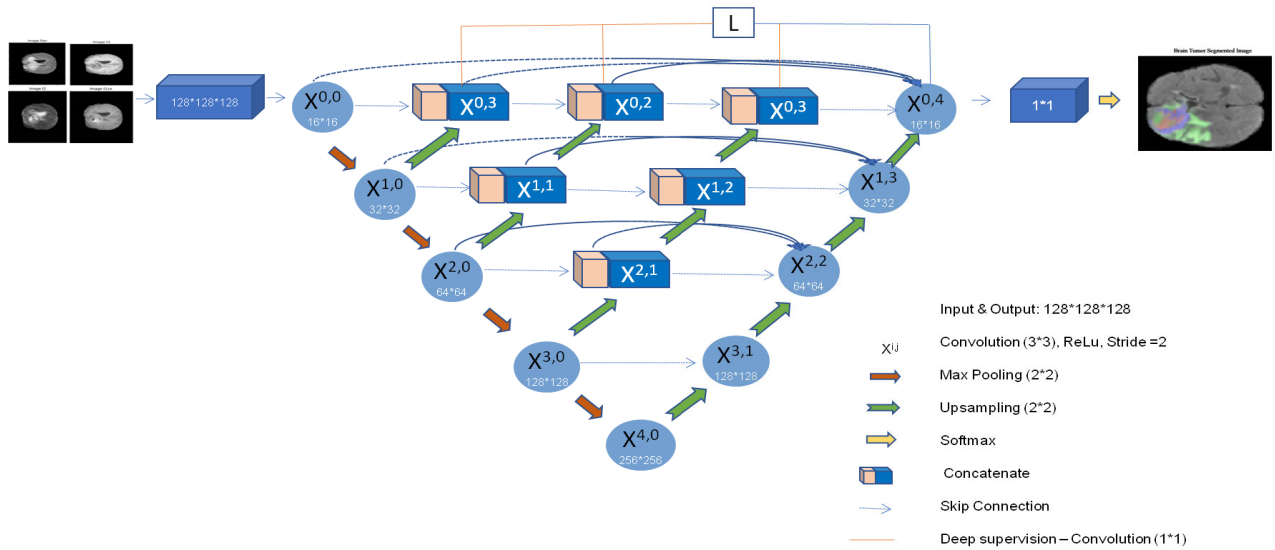
FIGURE 3. UNet++ architecture model.

TABLE 1. Parameters used for training model.

Parameters	Value
Input Size	128*128*128
Convolution Kernel size	3*3
Max pool size	2*2
Stride	2
Learning rate	0.001
No. of epochs	50
Batch size	1
Optimizer	Adam
Activation Function	Softmax
Loss	Categorical cross-entropy

purposes by determining numerous quantitative features through Radiomics feature extraction in medical images. Magnetic Resonance Imaging (MRI), Computed Tomography (CT) or Positron Emission Tomography (PET) scans can capture various aspects of these features.

PyRadiomics has become a widely-used open-source Python package that offers a broad set of functionalities for extracting radiomics features from medical images. It's become an essential tool for feature extraction with the collection of 1000 radiomics features like texture-based, intensity-based, wavelet-based, and higher-order features. Radiomics features were extracted individually for every tumor segmented image. To ensure consistency and eliminate noise or artifacts, preprocessing was necessary before the feature extraction of the images. Each resampled image was resized to fit the tumor mask's size. Wavelet and Log transform was employed to recover valuable data and enhance the tumor's edges with 3.0 as the Sigma value.

Normalization, Adaptive Histogram Equalization, Noise Calculation, Speckle noise and Laplace sharpening filters were also applied. As a result, 944 features were collected from each sample.

E. DATA AUGMENTATION

To proceed with the grading process, data augmentation has to be done to overcome the class imbalance. Followed by the segmentation process, 369 segmented images were available in each class, namely T1, T2, T1-CE and FLAIR. Out of 369 images, 76 images belong to LGG type and 293 images belong to HGG type of tumor class. Hence SMOTE and ADASYN upsampling techniques were employed to enhance the progress of the ML (Machine Learning) models and to decrease the bias in these classes. In this work, the most popular SMOTE and ADASYN upsampling techniques are used.

SMOTE methods wad introduced by Chawla et al. in 2002 [21]. SMOTE is one of the prevalent techniques for dealing with a class imbalance in machine learning models. To combat this problem, the SMOTE algorithm produces synthetic samples for the minority class, which balances the class distribution. This is achieved by creating current minority class samples in the feature space between new synthetic instances. In doing so, the machine learning model gains a more balanced and representative training set which leads to superior generalization and performance in the minority class.

The pseudocode of the SMOTE algorithm is explained in the Algorithm 1. This is applied to 369 samples in each modality. The number of samples increased in FLAIR, T1, T2 and T1-CE modalities using SMOTE are 581, 578, 574 and 576, respectively.

Algorithm 1 Pseudocode for SMOTE

Input:
    Samples of minority class
    Number of synthetic samples to generate
Output:
    Generated synthetic samples
for each sample in minority class do
    Locate the nearest neighbour samples
    Calculate the difference between a randomly selected
        sample and current sample
    Select a random number between 0 and 1
    Generate the new synthetic sample using the formula
        New synthetic sample = current sample + random
        *number * difference*
end for

ADASYN is an extension of the SMOTE algorithm proposed by He et al. in 2008, designed to address further the class imbalance problem in machine learning [22]. Both ADASYN and SMOTE create synthetic samples for the minority class.

Unlike SMOTE, ADASYN has an adaptive feature that concentrates on generating synthetic samples in areas with significant class imbalance. ADASYN adjusts synthetic sample generation by focusing on local density distributions in regions with greater class imbalance. This adaptive strategy enables ADASYN to effectively mitigate class imbalance problems, particularly in datasets with distinct degrees of class imbalance across different areas.

On applying the ADASYN Pseudocode shown in Algorithm 2 to 369 samples in each modality, the number of samples increased by 581 in FLAIR, 578 in T1, 579 in T2 and 568 in T1-CE modalities.

F. FEATURE SELECTION AND GRADING

Feature selection is a fundamental process to enhance the performance of machine learning models and reduce computational complexity. It is the process of selecting the relevant and essential features from a vast dataset. Here, from the extracted 944 features, a subset of relevant and informative features is chosen using the Tree-based feature selection method followed by PCA.

Tree-based feature selection is a technique for taking objective features based on decision tree algorithms. The essential 276 features from FLAIR, 238 from T1, 239 from T2 and 267 from T1-CE were selected in SMOTE method. While using the ADASYN method, 314 features from FLAIR, 299 from T1, 313 from T2 and 307 from T1-CE were selected.

Likewise, a statistical technique, PCA is employed to reduce the dimensionality. This technique can be helpful for pattern identification, data visualization, clustering, noise reduction and other data analysis tasks. In this task, 102 features from FLAIR, 92 from T1, 94 from T2 and

Algorithm 2 Pseudocode for ADASYN

Input:
 Samples of minority class
 Samples of majority class
 Number of synthetic samples to generate
Output:
Generated synthetic samples
for each sample in minority class do
  Calculate the ratio of class imbalance
      $d = S_{min} / S_{maj}$
      where S_{min} and S_{maj} are the number of
      minority and majority
      samples respectively.
Let d_{th} be the predefined maximum tolerated class
    imbalance threshold value
if $d < d_{th}$ then do
      Calculate the total number of examples to be
      generated for each minority sample
        $G = \beta (S_{min} - S_{maj})$
      where $\beta \in (0,1]$ is the parameter value that
      indicates the balance level. If $\beta = 1$, the class is
      perfectly balanced after generalization
      for each example $i = (1,\dots S_{min})$ in the current
      minority sample do
       Locate the k nearest neighbour and calculate
        $r_i = \Delta n / k$
      where Δn is the number of examples in k
      nearest neighbour i Normalize r_i as

$$\hat{r}_i = r_i / \sum_{i=1}^{S_{min}} r_i$$

      Calculate the number of synthetic examples to
      be generated for each minority sample as
        $G_i = \hat{r}_i * G$
      Generate G_i samples and append new samples
    end for
  end if
end for

---

83 from T1-CE were chosen for both SMOTE and ADASYN methods.

When it comes to medical imaging, grading brain tumors is crucial. To determine their malignancy or aggressiveness, these tumors are typically categorized into various groups. Some of the commonly used machine learning classification algorithms is explained as follows.

Support Vector Machine (SVM): A practical approach to this classification task is using SVM, a supervised learning algorithm. This algorithm is to identify an optimal hyperplane that effectively separates differing classes in the feature space. One of the commendable strengths of SVM is its ability to handle high-dimensional feature spaces, making them a viable option for brain tumor grading in conjunction with suitable features.

Decision Tree: One of the frequently used machine learning algorithm for grading or classification tasks is decision tree. The training data undergoes recursive splits into smaller subsets based on various features, intending to create subsets with similar grades.

Random Forests Method: Individual decision trees are combined to make predictions in the ensemble learning method known as random forests. The predictions of each tree, which is trained on distinct portions of the data, are aggregated to produce an outcome. With their ability to tackle both regression and classification tasks, random forests have earned a reputation for their resilience and capacity to detect intricate connections within datasets.

Stochastic Gradient Descent (SGD): The SGD Classifier is a classification algorithm that optimizes the model parameters using the stochastic gradient descent algorithm. Instead of updating based on the loss function gradient over a whole dataset, it focuses on a data point or mini-batch at each iteration. With this working strategy, this is computationally efficient for larger datasets.

These ML classifiers are exploited to classify Low-Grade Glioma (LGG) from High-Grade Glioma (HGG). Accuracy, Precision, Recall and F1score metrics are explored to evaluate and compare the performance of the classifiers.

G. SURVIVAL PREDICTION

Predicting brain tumor survival is an area where machine learning regression algorithms have proven their importance by predicting continuous numerical values based on input features. This method learns the relationship between the target variable and features from a dataset and makes predictions for new data. The most popular regression methods are described below.

Linear Regression: The widely used and simple model assumes a linear relationship between the target variable and input features. It decreases the variance of predicted values by fitting a line or hyperplane and minimizing the sum of squared differences between predicted and actual values.

Ridge Regression: Ridge regression is mainly used to minimize the variance of the model's predictions. It is employed to decrease overfitting the data.

Extreme Gradient Boost (XGBoost): This learning technique makes predictions by combining weak models. The feature space is recursively divided into regions by decision tree-based regression models, which are then assigned a constant value (average or median). This method can capture the intricate non-linear relationships and interactions between attributes, resulting in a tree structure.

In the proposed work, the ML-based regression models, namely Linear Regression, Ridge, SGD regressor and XGBoost regressor, were trained to predict the lifetime of brain tumor patients. As machine learning algorithms become better, their capacity to prognosticate brain tumor survival is sure to improve even further. The radiomics feature selection uses PCA to extract 89 features from FLAIR, 87 from T1, 83 from T2 and 75 from T1-CE. These models are evaluated with the predefined dataset value using Mean Square Error (MSE) and R-squared metrics.

H. EVALUATION METRICS

According to segmentation tasks, a pixel that aligns with the ground truth and is identified as belonging to a specific class is called a true positive (TP). By contrast, a true negative (TN) is a pixel properly recognized as not belonging to the specified class. Whenever the model inaccurately predicts a pixel as not part of a class, it's called a false positive (FP). In contrast, a false negative (FN) is where the model predicts a pixel to belong to the class inaccurately. Tumor classification tasks are similar, where TP denotes a correctly predicted tumor class that belongs to the given type. TN, in this regard, is the perfectly-identified part of a tumor as not in the given class. When the model inaccurately predicts a tumor class as belonging to a given class, it's called a false positive (FP). False negatives (FN) denote erroneous predictions of a class. The performance metrics employed in brain tumor segmentation and classification literature have been listed below.

Accuracy computes the correct identification of all classes or pixels, whether positive or negative and evaluates the ability of the model.

$$Accuracy = \frac{TP + TN}{TP + TN + FP + FN} \tag{1}$$

Sensitivity is the process of identifying positive samples/pixels among all real positive samples that determine how well the model performs this task.

$$Sensitivity = \frac{TP}{TP + FN} \tag{2}$$

Specificity relates to how many true negatives were correctly predicted compared to the actual negatives. This provides insight into the number of pixels or classes that could not be identified correctly.

$$Specificity = \frac{TN}{TN + FP} \tag{3}$$

Precision is a measure for predicting the accurate class/pixel by a model, revealing the proportion of positive predictions made correctly.

$$Precision = \frac{TP}{TP + FP} \tag{4}$$

Recall reveals the proportion of classes/pixels annotated in the ground truth that is also present in the model's prediction to describe the completeness of the model.

$$Recall = \frac{TN}{TP + FN} \tag{5}$$

F1-score effectively merges precision and recall into a harmonic mean to provide a balanced performance assessment.

$$F1Score = 2\frac{Precision * Recall}{(Precision + Recall)} \tag{6}$$

The Intersection over Union (IoU) or Jaccard index quantifies the overlap percentage between the predicted output of a model and the mask of the actual annotated truth.

$$IoU = \frac{TP}{TP + FP + FN} \tag{7}$$

IoU loss (Jaccard loss) is used in optimizing the segmentation metric and can be calculated by subtracting the IoU score from 1.

$$IoU \ (Jaccordloss) = 1 - IoU \tag{8}$$

Mean squared error (MSE) is measured by computing the mean squared difference between the predicted and real values.

$$MSE = \frac{1}{n}\sum\nolimits_{i=1}^{n}\left(yi - \acute{y}i\right)^2 \tag{9}$$

R-squared is a statistical indicator of how much variance in the dependent variable might be taken into account by the independent variables.

$$R^2 = 1 - \frac{\sum_i \left(yi - \acute{y}i\right)^2}{\sum_i \left(yi - \acute{y}\right)^2} \tag{10}$$

IV. RESULTS AND DISCUSSION

A. RESULTS OF UNet++ SEGMENTATION

The BraTS2020 MRI images were preprocessed and splitted into 80%, 10% and 10% for training, validation and testing datasets, respectively. UNet++ architecture model was implemented to train the training set MRI images. The saved model was then applied to segment the tumor in the validation and testing phase. Table 2 shows the outcome of the training, validation and testing phases. Accuracy, IOU score and Jaccard Loss are the metrics used to compute the improvement of the segmented model with the equations (1), (7) and (8), respectively.

TABLE 2. UNet++ segmentation results.

Parameters	Training	Validation	Testing
Accuracy	0.9825	0.9802	0.9881
Jaccard Loss	0.2433	0.2646	0.2517
IoU Score	0.7567	0.7354	0.7483

This proposed segmentation model obtained higher accuracy of 98%, an IoU score of 0.7483 greater than 0.5 (good score) and a Jaccard loss of 0.2517 in a testing phase. The graphical representation of these metrics in the testing phase is shown in Fig. 4.

1) COMPARISON OF SEGMENTATION MODELS
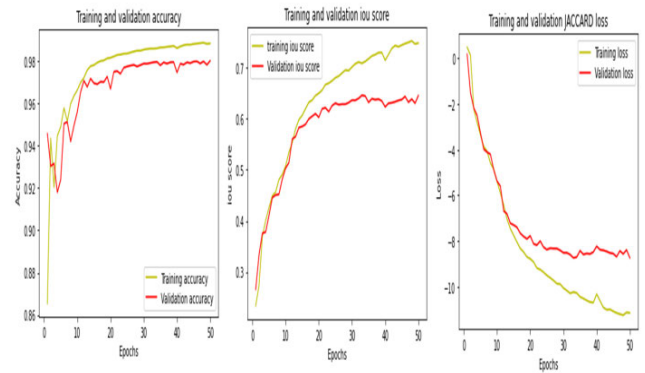The UNet++ model is compared with the well-known related segmentation models such as UNet, Attention UNet and

FIGURE 4. Graphical representation of accuracy, IoU score and jaccard loss.

ResNet50. The TP, FP, TN, and FN parameters of the confusion matrix were employed to determine the performance metrics. The parameters chosen to evaluate the segmentation results are Accuracy, Sensitivity Specificity and Precision which are measured using the equations (1), (2),(3) and (4), respectively. As shown in Table 3, UNet++ obtained the best values as 98.42%, 0.9947, 0.9858 and 0.9789 of Accuracy, Precision, Sensitivity and Specificity respectively.

TABLE 3. Comparison analysis of segmentation models.

MODEL	Accuracy(%)	Precision	Sensitivity	Specificity
UNet	97.76	0.9837	0.9786	0.9832
Attention UNet	96.41	0.9626	0.9692	0.9703
Resnet50	96.83	0.9725	0.9739	0.9625
UNet++	**98.42**	**0.9947**	**0.9858**	**0.9789**

B. EVALUATION AND COMPARISON OF CLASSIFIERS
As discussed in the above section, the SMOTE and ADASYN upsampling techniques were exploited after extracting 944 features using PyRadiomics. Instead of implementing all these features, Tree-based and PCA feature selection was done. Then the four classification machine learning algorithms were trained to classify the LGG and HGG classes. The experiment was done individually for SMOTE and ADASYN methods. The SGD classifier's confusion matrix and Area Under Curve (AUC) for FLAIR, T1, T2 and T1-CE modalities are shown in Fig.4 and Fig.5 for SMOTE and ADASYN methods, respectively.

Precision, Recall, and F1-score are widely used metrics for assessing classification models and are measured using the equations (4), (5) and (7), respectively. The obtained values for four classifiers are depicted in Table 4 while applying SMOTE technique. The SVM method gives a good F1-score of 0.93 on the FLAIR and 0.91 on the T1 modality. The SGD classifier yields 0.95 on the T2 and 0.91 on the T1-CE modality.

TABLE 4. Classification performance analysis for SMOTE technique with four grading classifiers.

		SVM			DT			RF			SGD		
		Precision	Recall	F1score	Precision	Recall	F1score	Precision	Recall	F1score	Precision	Recall	F1score
FLAIR	HGG	**0.95**	**0.92**	**0.93**	0.87	0.89	0.88	0.89	0.97	0.93	0.90	0.93	0.92
	LGG	**0.91**	**0.94**	**0.93**	0.87	0.85	0.86	0.96	0.87	0.91	0.92	0.89	0.91
T1	HGG	**0.93**	**0.89**	**0.91**	0.89	0.93	0.91	0.85	0.98	0.91	0.88	0.93	0.90
	LGG	**0.88**	**0.93**	**0.90**	0.92	0.87	0.90	0.98	0.80	0.88	0.92	0.85	0.88
T2	HGG	0.94	0.96	0.94	0.84	0.85	0.85	0.91	0.98	0.94	**0.94**	**0.97**	**0.95**
	LGG	0.95	0.91	0.93	0.83	0.81	0.82	0.98	0.89	0.93	**0.96**	**0.93**	**0.94**
T1-CE	HGG	0.89	0.91	0.90	0.92	0.85	0.88	0.89	0.96	0.93	**0.88**	**0.92**	**0.91**
	LGG	0.92	0.90	0.91	0.88	0.94	0.91	0.97	0.90	0.93	**0.93**	**0.89**	**0.91**

TABLE 5. Classification performance analysis for ADASYN technique with four grading classifiers.

|		SVM			DT			RF			SGD		
		Precision	Recall	F1score	Precision	Recall	F1score	Precision	Recall	F1score	Precision	Recall	F1score
FLAIR	HGG	**0.88**	**0.98**	**0.93**	0.78	0.93	0.85	0.86	1.00	0.92	0.83	0.98	0.90
	LGG	**0.98**	**0.89**	**0.93**	0.92	0.78	0.84	1.00	0.86	0.92	0.98	0.83	0.90
T1	HGG	0.79	0.96	0.87	0.81	0.87	0.84	0.87	0.95	0.90	**0.89**	**0.98**	**0.93**
	LGG	0.96	0.77	0.85	0.88	0.82	0.85	0.95	0.87	0.91	**0.98**	**0.89**	**0.93**
T2	HGG	**0.92**	**0.99**	**0.95**	0.80	0.85	0.82	0.90	0.95	0.93	0.92	0.98	0.94
	LGG	**0.98**	**0.91**	**0.95**	0.83	0.77	0.80	0.94	0.89	0.92	0.98	0.91	0.94
T1-CE	HGG	0.96	0.88	0.92	0.91	0.70	0.79	0.93	0.87	0.90	**1.00**	**0.92**	**0.96**
	LGG	0.88	0.96	0.92	0.74	0.93	0.82	0.86	0.93	0.89	**0.92**	**1.00**	**0.96**
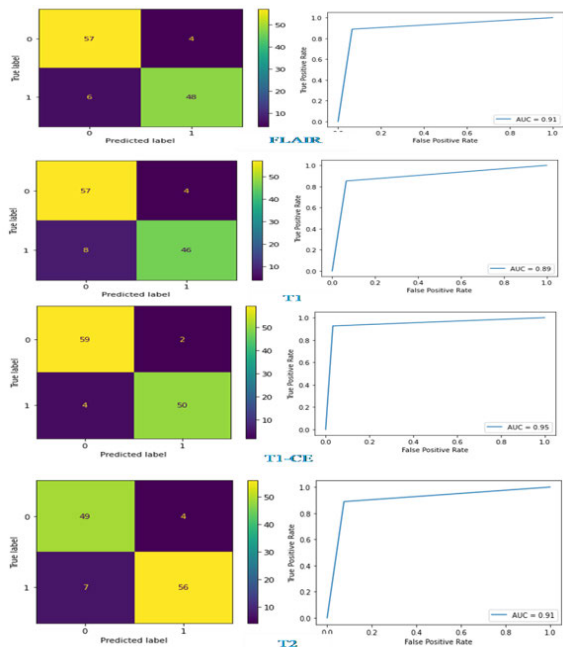
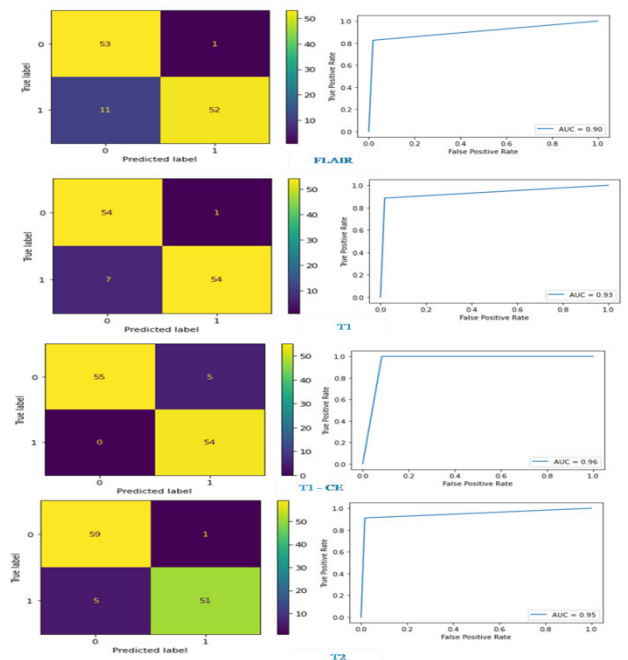**FIGURE 5.** SGD classifier's confusion matrix and AUC for SMOTE.

FIGURE 6. SGD classifier's confusion matrix and AUC for ADASYN.

Table 5 shows the classifier parameter values for the ADASYN method. In this case, SVM got the high F1-score on the FLAIR and T2 modality as 0.93 and 0.95, and SGD obtained 0.93 and 0.96 on the T1 and T1-CE modality.

The better result of 96% accuracy was acquired on T1-CE modality as compared with other modalities using the SGD classifier, as shown in Table 6.

TABLE 6. Accuracy comparison for smote and adasyn techniques.

Modality	SMOTE				ADASYN			
	SVM	DT	RF	SGD	SVM	DT	RF	SGD
FLAIR	0.93	0.87	0.92	0.91	0.93	0.85	0.92	0.90
T1	0.90	0.90	0.90	0.89	0.86	0.84	0.91	0.93
T2	0.95	0.83	0.94	0.91	0.95	0.81	0.92	0.95
T1-CE	0.91	0.90	0.93	0.95	0.92	0.81	0.89	**0.96**

C. EVALUATION OF SURVIVAL PREDICTION REGRESSION METHODS

Brain tumor survival was predicted using Linear, Ridge, SGD and XGBoost regression models. The 233 HGG-graded samples and PCA selected radiomics features were considered as input to the regressor models. The graphical representation for the four regression models of the FLAIR image is shown in Fig.7.
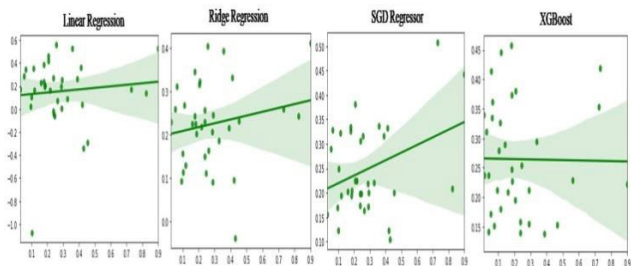
FIGURE 7. Graphical representation of regression models for FLAIR image.

Mean Square Error (MSE) and R-squared (R^2) values were calculated using the formula (9) and (10) to evaluate their performance. As shown in Table 7, the XGBoost regressor acquired the least MSE value and high R^2 value as 93726.45and 0.988, respectively.

TABLE 7. Survival prediction analysis of four regression methods.

Modality		Linear	Ridge	SGD	XGBoost
FLAIR	MSE	186413.72	205782.54	175693.69	**93726.45**
	R-squared	0.53	0.50	0.386	**0.988**
T1	MSE	197853.47	145792.54	139754.14	**96317.56**
	R-squared	0.496	0.439	0.319	**0.985**
T2	MSE	165431.23	156753.57	145669.57	**119713.47**
	R-squared	0.48	0.44	0.353	**0.982**
T1-CE	MSE	178952.41	157812.85	175269.53	**107459.25**
	R-squared	0.44	0.39	0.323	**0.985**

D. COMPARATIVE ANALYSIS OF THE PROPOSED METHOD WITH STATE-OF-THE-ART LITERATURE

To emphasize the outcomes of this paper work, it is contrasted against suggested start of the art methods for segmentation,

TABLE 8. Segmentation comparison analysis with literature models.

Reference	Segmentation Models	Accuracy (%)
[31]	CNN	81.35
[8]	2D CNN	88.20
[32]	UNet	89.60
[33]	CNN & SVM	97.10
[34]	ANN	98.00
[14]	DL with Attention mechanism	92.03
[35]	UNet& VGG16	98.00
[36]	CNN with Data Augmentation	96.50
[37]	3D-UNet	95.85
This Work	**Proposed UNet++ Model**	**98.81**

TABLE 9. Classification methods comparative analysis.

Reference	Grading Classifiers	Accuracy (%)
[24]	Random Forest	89.00
[38]	AdaBoost	89.90
[39]	Random Forest	88.00
[40]	Support Vector Machine	87.00
	3D CNN	96.49
[41]	3D UNet	90.00
[42]	Resnet-50	95.00
[43]	BrainMRNet	96.05
This Work	**Proposed SGD with ADASYN**	**96.87**

TABLE 10. Lifetime prediction comparative analysis with state of the art methods.

Reference	Lifetime Prediction Methods	MSE
[27]	Random Forest	6109105.6
	Multilayer Perceptron	5955021.1
[28]	Random Forest	268310.586
	Support Vector Machine	107569.325
	Multilayer Perceptron	102839.036
	XGBoost	127478.649
[44]	3D CNN	104773.00
[45]	Median Regression	101877.80
[29]	Random Forest	96470.98
This Work	**Proposed XGBoost Regressor**	**93726.45**

classification and survival prediction. The segmentation models are compared based on accuracy in Table 8.

In our proposed work, UNet++ model got higher accuracy of 98.42% which confirms its effectiveness in detecting the brain tumor pixels matched with ground truth regions. As depicted in the Table 9, SGD method with ADASYN data augmentation technique yields the higher accuracy of

96.87% that shows its prominence by evaluated against the already published machine learning classification techniques for grading. Table 10 records the performance analysis of the brain tumor survival prediction methods with literature techniques. When evaluated with the literature methods, XGBoost regression method achieved least MSE of 93726.45 on BraTS dataset.

V. CONCLUSION AND FUTURE WORK

This paper discusses the machine learning based MRI image analysis method for brain tumor segmentation, grading and lifetime prediction. The challenges involved in the segmentation of tumor portion include low contrast imaging, uncertainty in location, unclear boundary, and annotation in bias. In the proposed method, after exploring different segmentation architectures, we obtained a high accuracy of 98% using UNet++. The segmentation accuracy highly influences the model performance concerning grading and lifetime prediction. After performing radiomics feature extraction, SMOTE/ADASYN upsampling, feature selection and classification, we have obtained the highest accuracy of 96% for grading of LGG and HGG using SGD. The sequential procedure, as stated above, gives the best classification accuracy compared to the machine learning techniques in the literature. As stated in the literature, lifetime prediction accuracy using regression is significantly less due to various difficulties such as brain tumor heterogeneity, limited knowledge about tumor progression, individual variability in response to treatment and the development of secondary complications. We have obtained the MSE of 93726.45 using the XGBoost regression technique, which is a considerably good quantitative figure compared to the other methods in the literature. Though the proposed approach increases the classification and prediction accuracy with data augmentation and feature selection, there may be loss of in depth information. So recurrent neural network and different deep learning models can be exploited to facilitate the better performance and to reduce the information loss. Also many alternative benchmarking models would be used with explainable artificial intelligence (XAI) for improving the clarity of the models.

REFERENCES

[1] N. Sarshar, R. Ranjbarzadeh, S. J. Ghoushchi, and G. G. de Oliveira, "Glioma brain tumor segmentation in four MRI modalities using a convolutional neural network and based on a transfer learning method," in *Proc. 7th Brazilian Technol. Symp. (BTSym)*, 2023, pp. 386–402, doi: 10.1007/978-3-031-04435-9_39.

[2] J. Ferlay, H. Shin, F. Bray, D. Forman, C. Mathers, and D. M. Parkin, "Estimates of worldwide burden of cancer in 2008: GLOBOCAN 2008," *Int. J. Cancer*, vol. 127, no. 12, pp. 2893–2917, Dec. 2010, doi: 10.1002/ijc.25516.

[3] F. E. Bleeker, R. J. Molenaar, and S. Leenstra, "Recent advances in the molecular understanding of glioblastoma," *J. Neuro-Oncology*, vol. 108, no. 1, pp. 11–27, May 2012, doi: 10.1007/s11060-011-0793-0.

[4] D. N. Louis, A. Perry, P. Wesseling, D. J. Brat, I. A. Cree, D. Figarella-Branger, C. Hawkins, H. K. Ng, S. M. Pfister, G. Reifenberger, R. Soffietti, A. von Deimling, and D. W. Ellison, "The 2021 WHO classification of tumors of the central nervous system: A summary," *Neuro-Oncology*, vol. 23, no. 8, pp. 1231–1251, Aug. 2021, doi: 10.1093/neuonc/noab106.

[5] A. Wadhwa, A. Bhardwaj, and V. Singh Verma, "A review on brain tumor segmentation of MRI images," *Magn. Reson. Imag.*, vol. 61, pp. 247–259, Sep. 2019, doi: 10.1016/j.mri.2019.05.043.

[6] S. Jayade, D. T. Ingole, and M. D. Ingole, "Review of brain tumor detection concept using MRI images," in *Proc. Int. Conf. Innov. Trends Adv. Eng. Technol. (ICITAET)*, Dec. 2019, pp. 206–209, doi: 10.1109/ICITAET47105.2019.9170144.

[7] K. Sharma, A. Kaur, and S. Gujral, "Brain tumor detection based on machine learning algorithms," *Int. J. Comput. Appl.*, vol. 103, no. 1, pp. 7–11, Oct. 2014, doi: 10.5120/18036-6883.

[8] S. Bakas et al., "Identifying the best machine learning algorithms for brain tumor segmentation, progression assessment, and overall survival prediction in the BRATS challenge," 2019, *arXiv:1811.02629*.

[9] L. Liu, "Overall survival time prediction for high-grade glioma patients based on large-scale brain functional networks," *Brain Imag. Behav.*, vol. 13, pp. 1–19, Oct. 2019, doi: 10.1007/s11682-018-9949-2.

[10] D. Swain, S. K. Pani, and D. Swain, "A metaphoric investigation on prediction of heart disease using machine learning," in *Proc. Int. Conf. Adv. Comput. Telecommun. (ICACAT)*, Dec. 2018, pp. 1–6, doi: 10.1109/ICACAT.2018.8933603.

[11] J. Long, E. Shelhamer, and T. Darrell, "Fully convolutional networks for semantic segmentation," 2014, *arXiv:1411.4038*.

[12] O. Ronneberger, P. Fischer, and T. Brox, "U-net: Convolutional networks for biomedical image segmentation," 2015, *arXiv:1505.04597*.

[13] O. Oktay, J. Schlemper, L. Le Folgoc, M. Lee, M. Heinrich, K. Misawa, K. Mori, S. McDonagh, N. Y Hammerla, B. Kainz, B. Glocker, and D. Rueckert, "Attention U-net: Learning where to look for the pancreas," 2018, *arXiv:1804.03999*.

[14] R. Ranjbarzadeh, A. B. Kasgari, S. J. Ghoushchi, S. Anari, M. Naseri, and M. Bendechache, "Brain tumor segmentation based on deep learning and an attention mechanism using MRI multi-modalities brain images," *Sci. Rep.*, vol. 11, no. 1, p. 10930, May 2021, doi: 10.1038/s41598-021-90428-8.

[15] K. He, X. Zhang, S. Ren, and J. Sun, "Deep residual learning for image recognition," 2015, *arXiv:1512.03385*.

[16] C. Szegedy, W. Liu, Y. Jia, P. Sermanet, S. Reed, D. Anguelov, D. Erhan, V. Vanhoucke, and A. Rabinovich, "Going deeper with convolutions," in *Proc. IEEE Conf. Comput. Vis. Pattern Recognit. (CVPR)*, Jun. 2015, pp. 1–9, doi: 10.1109/CVPR.2015.7298594.

[17] K. He, X. Zhang, S. Ren, and J. Sun, "Deep residual learning for image recognition," in *Proc. IEEE Conf. Comput. Vis. Pattern Recognit. (CVPR)*, Nov. 2016, pp. 770–778, doi: 10.1109/CVPR.2016.90.

[18] Z. Zhou, M. Mahfuzur Rahman Siddiquee, N. Tajbakhsh, and J. Liang, "UNet++: A nested U-Net architecture for medical image segmentation," 2018, *arXiv:1807.10165*.

[19] R. J. Gillies, P. E. Kinahan, and H. Hricak, "Radiomics: Images are more than pictures, they are data," *Radiology*, vol. 278, no. 2, pp. 563–577, Feb. 2016, doi: 10.1148/radiol.2015151169.

[20] P. Kickingereder, S. Burth, A. Wick, M. Götz, O. Eidel, H.-P. Schlemmer, K. H. Maier-Hein, W. Wick, M. Bendszus, A. Radbruch, and D. Bonekamp, "Radiomic profiling of glioblastoma: Identifying an imaging predictor of patient survival with improved performance over established clinical and radiologic risk models," *Radiology*, vol. 280, no. 3, pp. 880–889, Sep. 2016, doi: 10.1148/radiol.2016160845.

[21] N. V. Chawla, K. W. Bowyer, L. O. Hall, and W. P. Kegelmeyer, "SMOTE: Synthetic minority over-sampling technique," *J. Artif. Intell. Res.*, vol. 16, pp. 321–357, Jun. 2002, doi: 10.1613/jair.953.

[22] H. He, Y. Bai, E. A. Garcia, and S. Li, "ADASYN: Adaptive synthetic sampling approach for imbalanced learning," in *Proc. IEEE Int. Joint Conf. Neural Netw. (IEEE World Congr. Comput. Intelligence)*, Jun. 2008, pp. 1322–1328, doi: 10.1109/IJCNN.2008.4633969.

[23] L. Breiman, "Random forests," *Mach. Learn.*, vol. 45, no. 1, pp. 5–32, Oct. 2001, doi: 10.1023/A:1010933404324.

[24] G. Latif, M. M. Butt, A. H. Khan, O. Butt, and D. N. F. A. Iskandar, "Multiclass brain glioma tumor classification using block-based 3D wavelet features of MR images," in *Proc. 4th Int. Conf. Electr. Electron. Eng. (ICEEE)*, Apr. 2017, pp. 333–337, doi: 10.1109/ICEEE2.2017.7935845.

[25] J. H. Friedman, "Greedy function approximation: A gradient boosting machine," *Ann. Statist.*, vol. 29, no. 5, pp. 1189–1232, Oct. 2001, doi: 10.1214/aos/1013203451.

[26] B. H. Menze et al., "The multimodal brain tumor image segmentation benchmark (BRATS)," *IEEE Trans. Med. Imag.*, vol. 34, no. 10, pp. 1993–2024, Oct. 2015, doi: 10.1109/TMI.2014.2377694.

[27] U. Baid, S. U. Rane, S. Talbar, and S. Gupta, "Overall survival prediction in glioblastoma with radiomic features using machine learning," *Frontiers Comput. Neurosci.*, vol. 14, p. 61, Jun. 2023. [Online]. Available: https://www.frontiersin.org/articles/10.3389/fncom.2020.00061

[28] M. Islam, V. Vs, V. J. M. Jose, N. Wijethilake, U. Utkarsh, and H. Ren, "Brain tumor segmentation and survival prediction using 3D attention UNet," 2021, *arXiv:2104.00985*.

[29] H. Huang, W. Zhang, Y. Fang, J. Hong, S. Su, and X. Lai, "Overall survival prediction for gliomas using a novel compound approach," *Frontiers Oncol.*, vol. 11, Aug. 2021, Art. no. 724191, doi: 10.3389/fonc.2021.724191.

[30] S. Bakas, "Advancing the cancer genome atlas glioma MRI collections with expert segmentation labels and radiomic features," *Sci. Data*, vol. 4, no. 1, p. 1, Sep. 2017, doi: 10.1038/sdata.2017.117.

[31] C. Zhou, S. Chen, C. Ding, and D. Tao, "Learning contextual and attentive information for brain tumor segmentation," in *Proc. 4th Int. Workshop*, Granada, Spain, Sep. 2019, pp. 497–507, doi: 10.1007/978-3-030-11726-9_44.

[32] S. Kumar, A. Negi, and J. N. Singh, "Semantic segmentation using deep learning for brain tumor MRI via fully convolution neural networks," in *Proc. ICTIS*, vol. 1, 2019, pp. 11–19, doi: 10.1007/978-981-13-1742-2_2.

[33] S. Deepak and P. M. Ameer, "Brain tumor classification using deep CNN features via transfer learning," *Comput. Biol. Med.*, vol. 111, Aug. 2019, Art. no. 103345, doi: 10.1016/j.compbiomed.2019.103345.

[34] Virupakshappa and B. Amarapur, "Correction to: Computer-aided diagnosis applied to MRI images of brain tumor using cognition based modified level set and optimized ANN classifier," *Multimedia Tools Appl.*, vol. 79, nos. 5–6, p. 3601, Feb. 2020, doi: 10.1007/s11042-018-6308-7.

[35] H. Rai and K. Chatterjee, "2D MRI image analysis and brain tumor detection using deep learning CNN model LeU-Net," *Multimedia Tools Appl.*, vol. 80, Nov. 2021, Art. no. 11504, doi: 10.1007/s11042-021-11504-9.

[36] E. U. Haq, H. Jianjun, K. Li, H. U. Haq, and T. Zhang, "An MRI-based deep learning approach for efficient classification of brain tumors," *J. Ambient Intell. Humanized Comput.*, vol. 14, no. 6, pp. 6697–6718, Oct. 2021, doi: 10.1007/s12652-021-03535-9.

[37] T. Ruba, R. Tamilselvi, and M. P. Beham, "Brain tumor segmentation in multimodal MRI images using novel LSIS operator and deep learning," *J. Ambient Intell. Humanized Comput.*, vol. 14, no. 10, pp. 13163–13177, Mar. 2022, doi: 10.1007/s12652-022-03773-5.

[38] A. Minz and C. Mahobiya, "MR image classification using Adaboost for brain tumor type," in *Proc. IEEE 7th Int. Advance Comput. Conf. (IACC)*, Jan. 2017, pp. 701–705, doi: 10.1109/IACC.2017.0146.

[39] H.-H. Cho, S.-H. Lee, J. Kim, and H. Park, "Classification of the glioma grading using radiomics analysis," *PeerJ*, vol. 6, p. e5982, Nov. 2018, doi: 10.7717/peerj.5982.

[40] H. Mzoughi, I. Njeh, A. Wali, M. B. Slima, A. BenHamida, C. Mhiri, and K. B. Mahfoudhe, "Deep multi-scale 3D convolutional neural network (CNN) for MRI gliomas brain tumor classification," *J. Digit. Imag.*, vol. 33, no. 4, pp. 903–915, Aug. 2020, doi: 10.1007/s10278-020-00347-9.

[41] P. Agrawal, N. Katal, and N. Hooda, "Segmentation and classification of brain tumor using 3D-UNet deep neural networks," *Int. J. Cognit. Comput. Eng.*, vol. 3, pp. 199–210, Jun. 2022, doi: 10.1016/j.ijcce.2022.11.001.

[42] P. Saxena, A. Maheshwari, S. Tayal, and S. Maheshwari, "Predictive modeling of brain tumor: A Deep learning approach," 2021, *arXiv:1911.02265*.

[43] M. Toğaçar, B. Ergen, and Z. Cömert, "BrainMRNet: Brain tumor detection using magnetic resonance images with a novel convolutional neural network model," *Med. Hypotheses*, vol. 134, Jan. 2020, Art. no. 109531, doi: 10.1016/j.mehy.2019.109531.

[44] M. Amian and M. Soltaninejad, "Multi-resolution 3D CNN for MRI brain tumor segmentation and survival prediction," in *Brainlesion: Glioma, Multiple Sclerosis, Stroke and Traumatic Brain Injuries* (Lecture Notes in Computer Science), vol. 11992, A. Crimi and S. Bakas, Eds. Cham, Switzerland: Springer, 2020, pp. 221–230, doi: 10.1007/978-3-030-46640-4_21.

[45] F. Kofler, "A baseline for predicting glioblastoma patient survival time with classical statistical models and primitive features ignoring image information," in *Brainlesion: Glioma, Multiple Sclerosis, Stroke and Traumatic Brain Injuries* (Lecture Notes in Computer Science), A. Crimi and S. Bakas, Eds. Cham, Switzerland: Springer, 2020, pp. 254–261, doi: 10.1007/978-3-030-46640-4_24.

M. RENUGADEVI received the B.Sc. degree in computer science from the Nadar Saraswathi College of Arts and Science, Theni, and the M.C.A. and M.Tech. degrees in computer science from SASTRA Deemed University, where she is currently pursuing the Ph.D. degree. She is also a Project Assistant with SASTRA Deemed University. Her research interests include medical imaging, machine learning, and deep neural networks.

K. NARASIMHAN received the M.Sc. degree in electronics from Bharathidasan University, the M.Tech. degree in nondestructive testing from the Regional Engineering College, Trichy, and the Ph.D. degree in medical image processing from SASTRA Deemed University, Thanjavur. He is currently a Senior Assistant Professor with the Department of ECE, School of EEE, SASTRA Deemed University. He has published more than 40 papers in reputed international journals and conferences. His research interests include digital image processing, medical image analysis, pattern recognition, and digital signal processing. He is a Life Member of the Indian Society of Systems for Science and Engineering (ISSE).

C. V. RAVIKUMAR received the M.Tech. degree in digital electronics and communication systems from Jawaharlal Nehru Technology University, Anatapur, in 2009, and the Ph.D. degree in communication networks from the Vellore Institute of Technology (VIT), Vellore, India, in 2018. He is currently an Assistant Professor SG with the Department of Embedded Technology, School of Electronics Engineering, VIT. His current research interests include communication networks, machine learning, deep learning, wireless sensor networks, and information security.

RAJESH ANBAZHAGAN (Senior Member, IEEE) received the B.Tech. and M.Tech. degrees in electronics and communication engineering from Pondicherry University, in 2005 and 2008, respectively, and the Ph.D. degree from the Department of Electronics Engineering, School of Engineering and Technology, Pondicherry University, in 2014. He was with Indian Telephone Industries (Government of India), from 2005 to 2006, Tata Consultancy Services, from 2008 to 2009, and VIT University, Vellore, from 2014 to 2020. He was a recipient of a gold medal at the PG Level from Pondicherry University and Pondicherry Engineering College. He has been awarded Innovation in Science Pursuit for Inspired Research (INSPIRE) Fellowship under assured opportunity for research career (AORC) from the Department of Science and Technology (DST), Ministry of Science and Technology (MST), Government of India. He was awarded by Google to perform foundational data, machine learning (ML), and artificial intelligence (AI) tasks and build secure networks. He is currently an Associate Professor with the School of Electrical and Electronics Engineering, SASTRA Deemed University, Thanjavur. His current research interests include 5G/6G networks, the IoT (industrial and medical), MIMO antennas, photonic crystal, localization of UAV and sensor networks, and emerging wireless networks.

GIOVANNI PAU (Member, IEEE) received the bachelor's degree in telematic engineering from the University of Catania, Italy, and the master's (cum laude) and Ph.D. degrees in telematic engineering from the Kore University of Enna, Italy. He is currently an Associate Professor with the Faculty of Engineering and Architecture, Kore University of Enna. He is the author/coauthor of more than 80 refereed papers published in journals and conference proceedings. His research interests include wireless sensor networks, fuzzy logic controllers, intelligent transportation systems, the Internet of Things, smart homes, and network security. He has been involved in several international conferences as the session co-chair and a technical program committee member. He serves/served as a leading guest editor in special issues for several international journals. He is an Editorial Board Member and an Associate Editor of several journals, such as IEEE Access, *Wireless Networks* (Springer), *EURASIP Journal on Wireless Communications and Networking* (Springer), *Wireless Communications and Mobile Computing* (Hindawi), *Sensors* (MDPI), and *Future Internet* (MDPI).

KANNAN RAMKUMAR was born in Madurai, India, in 1975. He received the B.Tech. degree in instrumentation and control engineering from Madurai Kamaraj University, in 1997, the M.Tech. degree from the Regional Engineering College, Trichy, in 2000, and the Ph.D. degree in control engineering from SASTRA Deemed University, India, in 2010. Since 1998, he has been with the Department of Electronics and Instrumentation, SASTRA Deemed University, where he was an Assistant Professor, became an Associate Professor, in 2011, and a Professor, in 2018. His current research interests include mobile robotics, estimation and control theory, and electrical drive systems. He has received funding from DRDO, an Indian government defense agency, for investigating the localization and mapping problem in mobile robot. He was the Chair Professor of Wipro Mission 10X, a pedagogy skills improvement initiative in SASTRA University (2011–2012). He was a recipient of the prestigious "Innovative Practitioner" a teaching excellence award from Wipro for the year 2011. Currently, he is solving machine learning, estimation, and control problems related to applications like electric vehicle, mobile robots, and process control. He is also heading the Control Artificial Intelligence, Biomedical and Robotics Engineering (CALIBRE), a research group.

MOHAMED ABBAS received the B.Sc. degree in electronics engineering from the Faculty of Engineering, Mansoura University, Egypt, in 1998, and the M.Sc. and Ph.D. degrees in computer engineering from Mansoura University, in 2002 and 2008, respectively. Since this date, he has was an Assistant Professor with the Department of Communications and Computer Engineering, College of Engineering, Delta University. He is currently an Associate Professor with the Department of Electrical Engineering, King Khaled University, Abha, Saudi Arabia. His research interests include intelligent systems, medical informatics, nanotechnology, biological signaling, and bioinformatics.

N. RAJU received the Ph.D. degree from SASTRA Deemed University, India, in 2018, the master's degree in applied electronics from Anna University, and the master's Diploma degree in VLSI from C-DAC. He is currently a Senior Assistant Professor with SASTRA Deemed University. He has a teaching experience of 20 years. His research interests include speech processing, embedded systems, FPGA, and the IoT. He has published more than 30 papers in national and international journals.

K. SATHISH received the master's degree in communication systems from Jawaharlal Nehru Technology University, Anantapur, India, in 2017. He is currently a Research Scholar with the School of Electronics Engineering, Vellore Institute of Technology, Vellore, Tamil Nadu, India. His research interests include underwater wireless sensor networks, 5G communications, machine learning, and artificial intelligence.

PRABU SEVUGAN (Senior Member, IEEE) received the B.Eng. degree in CSE and the double M.Tech. and Ph.D. degrees in remote sensing and CSE. He is currently a certified blockchain associate professor. He was a Postdoctoral Fellow with the Department of Computer Science and Engineering, IIT Bombay. He was a Professor and the Head of the Department of Information Security, School of Computer Science and Engineering, VIT Vellore. He is also an Associate Professor with the Department of Banking Technology, Pondicherry University (A Central University), Puducherry, India. He guided eight Ph.D.'s and one M.S. (by Research). He acquired research grants worth 2.4 Cr. He has more than 130 publications in peer-reviewed journals and conferences, edited four books, published 16 book chapters, and one patent. He has organized three international conferences which include one IEEE conference as the chair and also participated in many workshops and seminars. He is having more than 19 years of experience in teaching and research. He is a member of many professional bodies.

• • •